Electronic Supplementary Material (ESI) for Inorganic Chemistry Frontiers.

Construction of brown mesoporous carbon nitride with wide spectral response for high performance photocatalytic H_2 evolution

Jinzhou Chen[a], Xianglin Zhu[a,*], Zhifeng Jiang[a], Wei Zhang[a], Haiyan Ji[a,*], Xingwang Zhu[a], Yanhua Song[b], Zhao Mo[a], Huaming Li[a], and Hui Xu[a,*]

[a] *School of Materials Science and Engineering, Institute for Energy Research, Jiangsu University, Zhenjiang, Jiangsu 212013, P.R. China*

[b] *School of Environmental and Chemical Engineering, Jiangsu University of Science and Technology, Zhenjiang, Jiangsu, 212003, PR China*

*Corresponding author:

E-mail: zhuxl@ujs.edu.cn (X. Zhu), hyji1013@ujs.edu.cn (H. Ji), xh@ujs.edu.cn (H. Xu)

Experimental

Preparation of 2D CN

2D CN was prepared by two-step calcination and thermal exfoliation method. Briefly, 10g of urea was calcined to 550 °C at a heating rate of 10 °C/min and maintained for 4 hours. After it was naturally cooled to room temperature, the mixture was grounded in an alumina crucible to get the uniform bulk carbon nitride. The bulk carbon nitride was calcined at 550 °C for 0.5h, and then took out after cooling down to the room temperature. The obtained light-yellow powder was 2D CN (yield≈37.5%). It should be noted that in order to ensure the repeatability of the experiment, we did not blindly pursue to obtain single or few layers of ultra-thin carbon nitride. .

Preparation of BMCN

The brown mesoporous carbon nitride was synthesized through calcining the mixture of the 2D CN and NaH_2PO_2 at certain temperatures. In details, 100 mg 2D CN and certain amounts of NaH_2PO_2 were ground thoroughly to get a uniform mixture, then the mixture was heated to 425 °C under the argon atmosphere and kept for one hour. The obtained sample was washed with water and alcohol for several times to remove impurities. The mesoporous brown carbon nitride was obtained after a vacuum drying progress for an overnight. According to the amount of the used NaH_2PO_2, the final prepared brown

mesoporous carbon nitride photocatalysts were named as BMCN-X in which X indicated the quality of NaH_2PO_2.

Photoelectrochemical measurement

A certain amount of sample was weighed and dispersed in water under ultrasonic to get a uniform 1mg/mL suspension. Then, 50μL of the suspension was dropped onto a piece of 0.5 cm^2 (1 cm × 0.5 cm) indium tin oxide (ITO)-coated with a pipette. Working electrodes were got after the suspension was dried under the infrared lamp irradiation. The photocurrents of the samples were tested on the CHI660 B electrochemical analyzer (Shanghai Chenhua, China) under a 500W Xe lamp irradiation. Ag/AgCl (saturated KCl solution), and platinum (Pt) wire were used as the reference electrode, and the counter electrode, respectively. The working potential was −0.3 V (vs. Ag/AgCl).

Photocatalytic activity measurement

10 mg of the catalyst was dispersed in the 100 ml solution of water and triethanolamine (TEOA), and the volume ration of water: TEOA is 9:1. The fresh prepared chloroplatinic acid solution was used as the Pt source and the loading amount was 3%. The reactor was under ultrasonic treatment for 15 minutes to get a uniform suspension. The photocatalytic H_2 production experiments were carried out by using a 300W Xe lamp equipped with a 420 nm cut-off filter ($\lambda \geq 420$nm) under vacuum.

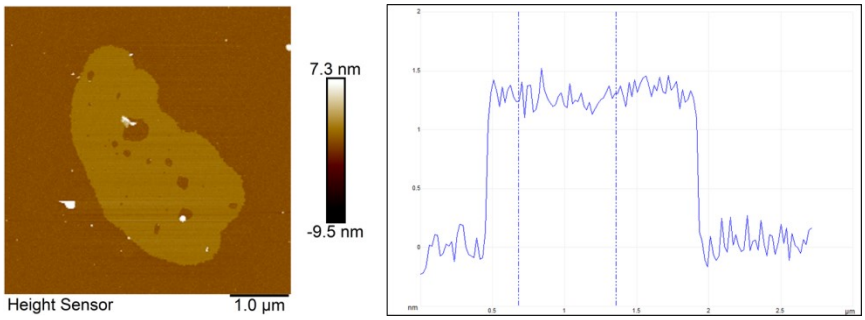

Figure S1. AFM results of the 2D CN.

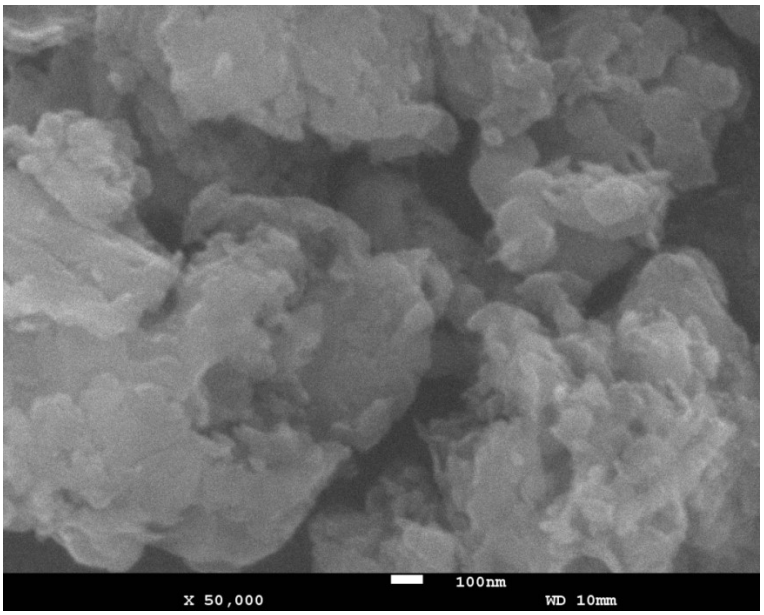

Figure S2. The SEM image of the bulk carbon nitride

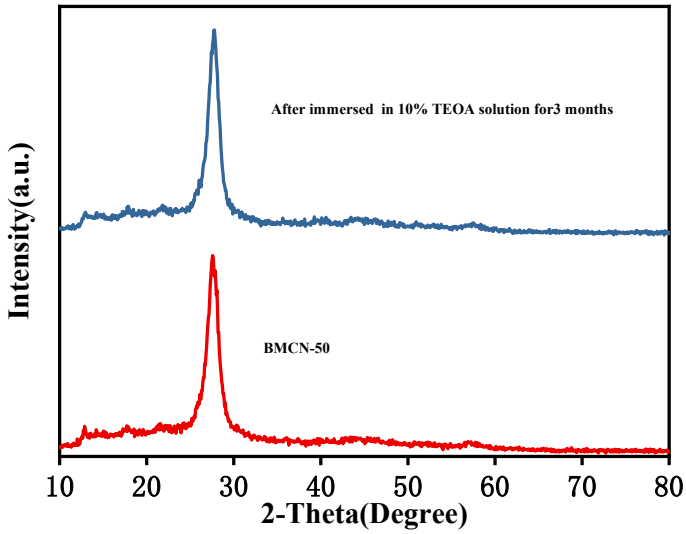

Figure S3. XRD results of the BMCN-50 after being immersed in 10% TEOA solution for 3 months. It demonstrated that the XRD has no obvious change after the BMCN-50 was immersed in 10% TEOA solution for 3 months.

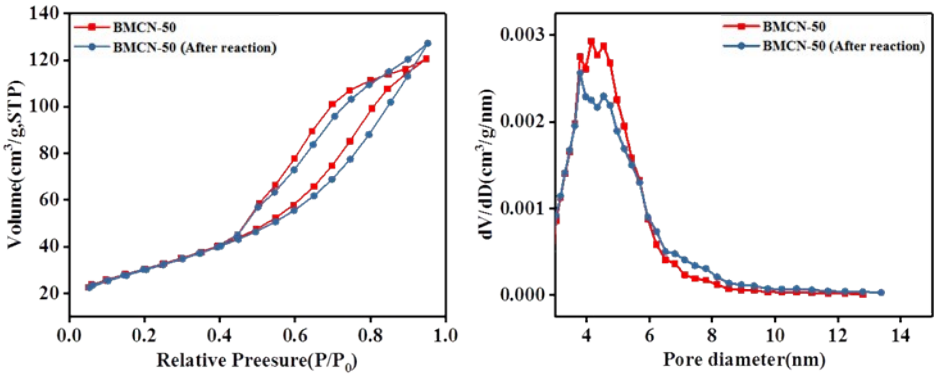

Figure S4. N_2 adsorption-desorption isotherms curves and pore size distribution curves of BMCN-50 after photocatalytic reaction

The N_2 adsorption-desorption isotherms curve of BMCN-50 after photocatalytic reaction still remains Type Ⅳa (mesopores, Cylindrical pore shape). The BET surface area of BMCN-50 after photocatalytic reaction is 109.69m^2/g. The pore size distribution of BMCN-50 after photocatalytic reaction is similar to that of pristine BMCN-50. The pore volume of pristine BMCN-50 and BMCN-50 after photocatalytic reaction is 0.171 and 0.177cm^3/g respectively.

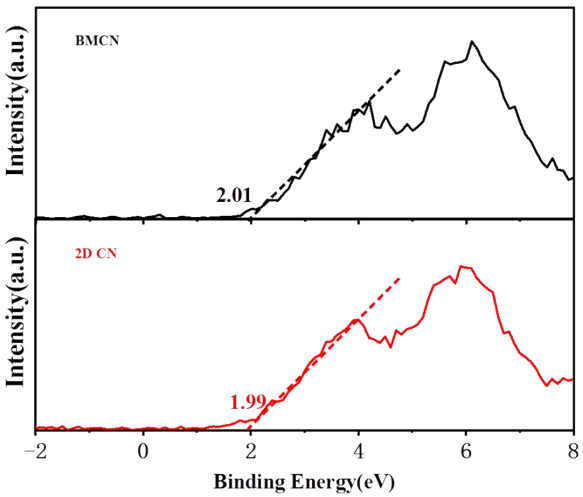

Figure S5. XPS valence band spectrum of 2D CN and BMCN-50.

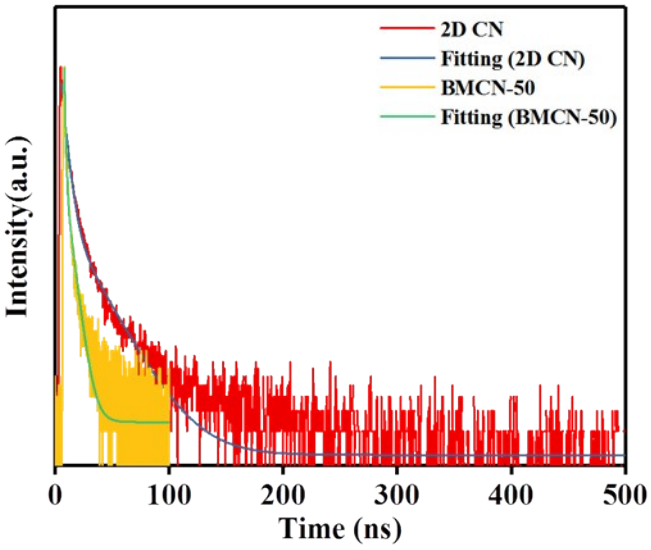

Figure S6. TRPL decay spectra of 2D CN and BMCN-50

Average lifetime of two specimens is calculated according to the following formula:

$$\tau_{av} = a_1\tau_1 + a_2\tau_2$$

*τ_1 and τ_2 are lifetime; a_1 and a_2 are normalized pre-exponential factors.

The average lifetime of BMCN-50 decreases to 2.73ns, almost a quarter of 2D CN' average lifetime. (9.84ns)

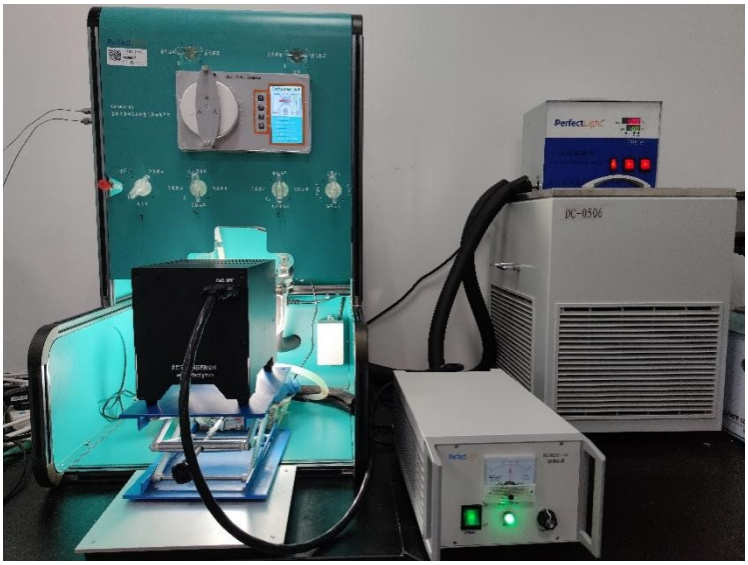

Figure S7. Photograph of Full glass automatic on-line trace gas analysis system (Labsolar-6A, Beijing

Perfectlight)

Calculation of apparent quantum yield

*The apparent quantum yield (AQY) was measured by inserting an appropriate band pass filter in front light source. And the other conditions are similar to the one for hydrogen evolution measurement.

The radius of light spot is 1 cm

The area of light spot is 3.14 cm^2

The average light intensity is determined as follows:

$$E = \frac{E_{centre}}{3} + 2 \times \frac{(E_{edge1} + E_{edge2} + E_{edge3} + E_{edge4})/4}{3}$$

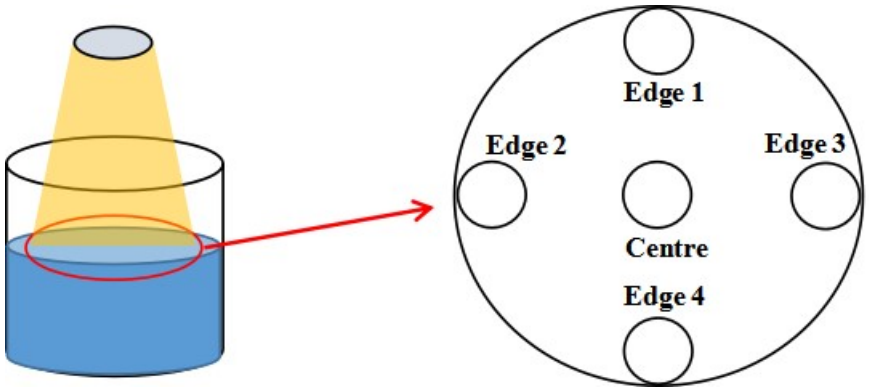

Schematic illustrations of the illuminated photocatalyst area in particle suspension

wavelength	H_2 Evolved of 2D CN	H_2 Evolved of BMCN-50	AQY Of 2D CN	AQY of BMCN-50
λ= 420nm	32.89μmol	42.26μmol	3.23%	4.15%
λ= 435nm	9.93μmol	43.16μmol	0.92%	4.00%
λ= 450nm	2.48μmol	39.73μmol	0.22%	3.52%
λ= 550nm	0μmol	0.72μmol	0%	0.50%

Take BMCN-50 as an example:

λ=420 nm:

$$N = \frac{E\lambda}{hc} = \frac{53.72 \times 10^{-3} \times 3 \times 3600 \times 420 \times 10^{-9}}{6.626 \times 10^{-34} \times 3 \times 10^{8}} = 12.26 \times 10^{20}$$

$$AQE = \frac{the\ number\ of\ reacted\ electrons}{the\ number\ of\ incident\ photons} \times 100\%$$
$$= \frac{2 \times the\ number\ of\ evolved\ H_2\ molecules}{N} \times 100\%$$
$$= \frac{2 \times 6.02 \times 10^{23} \times 42.26 \times 10^{-6}}{12.26 \times 10^{20}} \times 100\% = 4.15\%$$

λ=435 nm:

$$N = \frac{E\lambda}{hc} = \frac{54.98 \times 10^{-3} \times 3 \times 3600 \times 435 \times 10^{-9}}{6.626 \times 10^{-34} \times 3 \times 10^{8}} = 12.99 \times 10^{20}$$

$$AQE = \frac{the\ number\ of\ reacted\ electrons}{the\ number\ of\ incident\ photons} \times 100\%$$
$$= \frac{2 \times the\ number\ of\ evolved\ H_2\ molecules}{N} \times 100\%$$
$$= \frac{2 \times 6.02 \times 10^{23} \times 43.16 \times 10^{-6}}{12.99 \times 10^{20}} \times 100\% = 4.00\%$$

λ=450 nm:

$$N = \frac{E\lambda}{hc} = \frac{55.45 \times 10^{-3} \times 3 \times 3600 \times 450 \times 10^{-9}}{6.626 \times 10^{-34} \times 3 \times 10^{8}} = 13.56 \times 10^{20}$$

$$AQE = \frac{the\ number\ of\ reacted\ electrons}{the\ number\ of\ incident\ photons} \times 100\%$$
$$= \frac{2 \times the\ number\ of\ evolved\ H_2\ molecules}{N} \times 100\%$$
$$= \frac{2 \times 6.02 \times 10^{23} \times 39.73 \times 10^{-6}}{13.58 \times 10^{20}} \times 100\% = 3.52\%$$

λ=550 nm:

$$N = \frac{E\lambda}{hc} = \frac{61.31\times10^{-3}\times3\times3600\times550\times10^{-9}}{6.626\times10^{-34}\times3\times10^{8}} = 18.32\times10^{20}$$

$$AQE = \frac{the\ number\ of\ reacted\ electrons}{the\ number\ of\ incident\ photons}\times100\%$$
$$= \frac{2\times the\ number\ of\ evolved\ H_2\ molecules}{N}\times100\%$$
$$= \frac{2\times6.02\times10^{23}\times0.72\times10^{-6}}{18.32\times10^{20}}\times100\% = 0.05\%$$

The comparison of activity and apparent quantum yield of the reported g-C_3N_4-based photocatalysts.

Photocatalyst	Reaction condition	BET	AQY	Ref.
BMCN	**3 wt% Pt co-catalyst 10% TEOA solution 10 mg catalyst**	**109.822 m^2/g**	**4.15% (420 nm) 4% (435 nm) 3.52% (450 nm) 0.5% (550 nm)**	**This work**
PtS_2/MCN	1 wt% PtS_2 co-catalyst 10% TEOA solution 50 mg catalyst	110.69 m^2/g	0.7% (420 nm) 0.38% (450 nm)	1
RPCN	3 wt% Pt co-catalyst 10% TEOA solution 20 mg catalyst	13.8 m^2/g	13% (500 nm) 0.84% (700 nm)	2

CNN/BDCNN	0.9wt% Pt and 3 wt% $Co(OH)_2$ co-catalyst Ultrapure water 20 mg catalyst	CNN: 179.33 m^2/g BDCNN: 227.69 m^2/g	4.59% (420 nm) 2.61% (425 nm) 1.07% (450 nm) 0.34% (500 nm)	3
CoP/g-C_3N_4	3 wt% CoP co-catalyst 15% TEOA solution, 50 mg catalyst	N/A	12.4 % (420 nm) 7.5 % (440 nm) 3.8 % (460 nm)	4
NiL/CN-DAPS	0.3g $NiCl_2.6H_2O$ 10% TEOA solution 50 mg catalyst	N/A	2.15% (450 nm)	5
C_{ring}-C_3N_4	3 wt% Pt co-catalyst Ultrapure water 10 mg catalyst	N/A	5 % (420 nm)	6
CDots-C_3N_4	80 mg catalyst	N/A	16% (420 nm) 6.29% (580 nm) 4.42% (600 nm)	7
porous PCN-S	1 wt% Pt co-catalyst 20% TEOA solution 50 mg catalyst	122.6 m^2/g	3.56% (420 nm)	8
S-CN	3 wt% Pt co-catalyst 10% TEOA	160 m^2/g	0.8% (420 nm)	9

	solution 20 mg catalyst			
g-C_2N_3	0.35mol/L Na_2S and 0.25mol/L Na_2SO_3 50 mg catalyst	N/A	19.9% (420 nm)	10
g-C_3N_4 nanotubes	3 wt% Pt co-catalyst 10% TEOA solution 10 mg catalyst	127.8 m^2/g	6.8% (420 nm)	11
R-TCN	3 wt% Pt co-catalyst 10% TEOA solution 10 mg catalyst	53.14 m^2/g	1.9% (420 nm)	12
Carbon Nitride Needles	3 wt% Pt co-catalyst 3% TEOA solution 20 mg catalyst	185 m^2/g	1% (420 nm)	13
MnO_2/monolayer CN	3 wt% Pt co-catalyst 20 mg catalyst	N/A	23.33% (420 nm) 9.49% (435 nm) 1.04% (450 nm)	14
Nax-CNNTs	3 wt% Pt co-catalyst 10% TEOA	94 m^2/g	1.8% (420 nm)	15

	solution 20 mg catalyst			
High-crystalline g-C_3N_4 nanosheets	3 wt% Pt co-catalyst 10% TEOA solution 100 mg catalyst	39.24 m^2/g	6.17% (420 nm)	16
holey g-C_3N_4 nanosheets	3 wt% Pt co-catalyst 10% TEOA solution 50 mg catalyst	95.04 m^2/g	2.1% (420 nm)	17
P-TCN	1 wt% Pt co-catalyst 20% TEOA solution 30 mg catalyst	13.38 m^2/g	5.68% (420 nm)	18
NP550	1 wt% Pt co-catalyst 20% TEOA solution 50 mg catalyst	7.8 m^2/g	1.6% (420 nm)	19
CQD-implanted g-C_3N_4 nanotubes	3 wt% Pt co-catalyst 25% methanol solution 50 mg catalyst	119.942 m^2/g	10.94% (420 nm)	20

References

1. Liu, J.; Xu, H.; Yan, J.; Huang, J.; Song, Y.; Deng, J.; Wu, J.; Ding, C.; Wu, X.; Yuan, S.; Li, H., Efficient photocatalytic hydrogen evolution mediated by defect-rich 1T-PtS_2 atomic layer nanosheet modified mesoporous graphitic carbon nitride. *J. Mater. Chem. A* **2019,** *7* (32), 18906-18914.

2. Xu, Y.; Fan, M.; Yang, W.; Xiao, Y.; Zeng, L.; Wu, X.; Xu, Q.; Su, C.; He, Q., Homogeneous Carbon/Potassium-Incorporation Strategy for Synthesizing Red Polymeric Carbon Nitride Capable of Near-Infrared Photocatalytic H_2 Production. *Adv. Mater.* **2021**.

3. Zhao, D.; Wang, Y.; Dong, C.-L.; Huang, Y.-C.; Chen, J.; Xue, F.; Shen, S.; Guo, L., Boron-doped nitrogen-deficient carbon nitride-based Z-scheme heterostructures for photocatalytic overall water splitting. *Nat. Energy* **2021,** *6* (4), 388-397.

4. Li, C.; Du, Y.; Wang, D.; Yin, S.; Tu, W.; Chen, Z.; Kraft, M.; Chen, G.; Xu, R., Unique PCoN Surface Bonding States Constructed on g-C_3N_4 Nanosheets for Drastically Enhanced Photocatalytic Activity of H_2 Evolution. *Adv. Funct. Mater.* **2017,** *27* (4).

5. Zhang, Y.-X.; Zeng, P.; Yu, Y.-X.; Zhang, W.-D., Integration of nickel complex as a cocatalyst onto in-plane benzene ring-incorporated graphitic carbon nitride nanosheets for efficient photocatalytic hydrogen evolution. *Chem. Eng. J.* **2020,** *381*.

6. Che, W.; Cheng, W.; Yao, T.; Tang, F.; Liu, W.; Su, H.; Huang, Y.; Liu, Q.; Liu, J.; Hu, F.; Pan, Z.; Sun, Z.; Wei, S., Fast Photoelectron Transfer in C_{ring}-C_3N_4 Plane Heterostructural Nanosheets for Overall Water Splitting. *J. Am. Chem.Soc.* **2017,** *139* (8), 3021-3026.

7. Liu, J.; Liu, Y.; Liu, N.; Han, Y.; Zhang, X.; Huang, H.; Lifshitz, Y.; Lee, S.-T.; Zhong, J.; Kang, Z., Metal-free efficient photocatalyst for stable visible water splitting via a two-electron pathway. *Science* **2015,** *347* (6225), 970-974.

8. Ran, J.; Ma, T. Y.; Gao, G.; Du, X.-W.; Qiao, S. Z., Porous P-doped graphitic carbon nitride nanosheets for synergistically enhanced visible-light photocatalytic H_2 production. *Energ. Environ. Sci.* **2015,** *8* (12), 3708-3717.

9. Chen, Y.; Wang, X., Template-Free Synthesis of Hollow G-C_3N_4 Polymer with Vesicle Structure for Enhanced Photocatalytic Water Splitting. *J. Phys.Chem. C* **2018,** *122* (7), 3786-3793.

10. Tang, D.; Shao, C.; Jiang, S.; Sun, C.; Song, S., Graphitic C_2N_3: An Allotrope of g-C_3N_4 Containing Active Azide Pentagons as Metal-Free Photocatalyst for Abundant H_2 Bubble Evolution. *Acs Nano* **2021,** *15* (4), 7208-7215.

11. Mo, Z.; Xu, H.; Chen, Z.; She, X.; Song, Y.; Wu, J.; Yan, P.; Xu, L.; Leia, Y.; Yuan, S.; Li, H., Self-assembled synthesis of defect-engineered graphitic carbon nitride nanotubes for efficient conversion of solar energy. *Appl. Catal.B-Environ.* **2018,** *225*, 154-161.

12. Ge, G.; Guo, X.; Song, C.; Zhao, Z., Reconstructing Supramolecular Aggregates to Nitrogen-Deficient g-C_3N_4 Bunchy Tubes with Enhanced Photocatalysis for H_2 Production. *Acs Appl. Mater. Inter.* **2018,** *10* (22), 18746-18753.

13. Barrio, J.; Lin, L.; Amo-Ochoa, P.; Tzadikov, J.; Peng, G.; Sun, J.; Zamora, F.; Wang, X.; Shalom, M., Unprecedented Centimeter-Long Carbon Nitride Needles: Synthesis, Characterization and Applications. *Small* **2018,** *14* (21).

14. Mo, Z.; Xu, H.; Chen, Z.; She, X.; Song, Y.; Lian, J.; Zhu, X.; Yan, P.; Lei, Y.; Yuan, S.; Li, H., Construction of MnO_2/Monolayer g-C_3N_4 with Mn vacancies for Z-scheme overall water splitting. *Appl. Catal.B-Environ.* **2019,** *241*, 452-460.
15. Zhang, L.; Ding, N.; Hashimoto, M.; Iwasaki, K.; Chikamori, N.; Nakata, K.; Xu, Y.; Shi, J.; Wu, H.; Luo, Y.; Li, D.; Fujishima, A.; Meng, Q., Sodium-doped carbon nitride nanotubes for efficient visible light-driven hydrogen production. *Nano Res.* **2018,** *11* (4), 2295-2309.
16. Xing, W.; Tu, W.; Han, Z.; Hu, Y.; Meng, Q.; Chen, G., Template-Induced High-Crystalline g-C_3N_4 Nanosheets for Enhanced Photocatalytic H_2 Evolution. *Acs Energy Letters* **2018,** *3* (3), 514-519.
17. Liu, Q.; Wang, X.; Yang, Q.; Zhang, Z.; Fang, X., A novel route combined precursor-hydrothermal pretreatment with microwave heating for preparing holey g-C_3N_4 nanosheets with high crystalline quality and extended visible light absorption. *Appl. Catal.B-Environ.* **2018,** *225*, 22-29.
18. Liu, B.; Ye, L.; Wang, R.; Yang, J.; Zhang, Y.; Guan, R.; Tian, L.; Chen, X., Phosphorus-Doped Graphitic Carbon Nitride Nanotubes with Amino-rich Surface for Efficient CO_2 Capture, Enhanced Photocatalytic Activity, and Product Selectivity. *Acs Appl. Mater. Inter.* **2018,** *10* (4), 4001-4009.
19. Cheng, J.; Hu, Z.; Lv, K.; Wu, X.; Li, Q.; Li, Y.; Li, X.; Sun, J., Drastic promoting the visible photoreactivity of layered carbon nitride by polymerization of dicyandiamide at high pressure. *Appl. Catal.B-Environ.* **2018,** *232*, 330-339.
20. Wang, Y.; Liu, X.; Liu, J.; Han, B.; Hu, X.; Yang, F.; Xu, Z.; Li, Y.; Jia, S.; Li, Z.; Zhao, Y., Carbon Quantum Dot Implanted Graphite Carbon Nitride Nanotubes: Excellent Charge Separation and Enhanced Photocatalytic Hydrogen Evolution. *Angew. Chem.-Int. Edit.* **2018,** *57* (20), 5765-5771.